Global NEST Journal, Vol 26, No 7, 06164

Spatial characteristic of carbon emission intensity under "dual carbon" targets: Evidence from China

Gang Zeng[1]*, Yi Guo[1], Song Nie[3], Keyan Liu[2], Yue Cao[2], Ling Chen[1], Dezhe Ren[1], Jiaqi Zhang[1] and Bowen Yan[2]
[1]School of Economics and Management, Civil Aviation University of China, Tianjin, 300300, China
[2]School of Transportation Science and Engineering, Civil Aviation University of China, Tianjin, 300300, China
[3]School of Economics, Nankai University, Tianjin, 300071, China
Received: 11/05/2024, Accepted: 14/06/2024, Available online: 10/07/2024
*to whom all correspondence should be addressed: e-mail: gzeng666@foxmail.com
https://doi.org/10.55555/gnj.006164

Graphical abstract

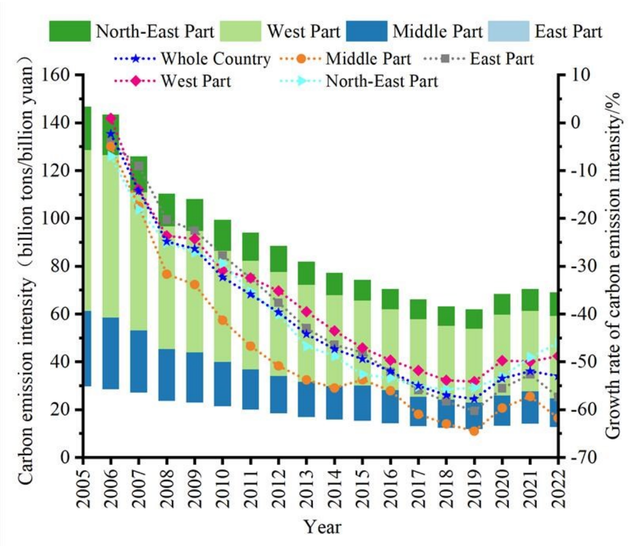

Abstract

Reducing carbon emissions is one of the important ways to achieve the goal of "dual carbon". Taking carbon emission intensity as the research object, this paper analyzes the spatial effects of carbon emission intensity at provincial level in China during 2005-2022 by kaya extended model, standard deviation ellipse, Theil index and kernel density analysis model. The results show that: (1) Overall, the distribution of carbon emission intensity in China exhibits distinct regional characteristics, with significant heterogeneity in emissions among regions. (2) With advancements in technology and economy, China's carbon emission intensity has shown a downward trend, albeit with a U-shaped fluctuation. (3) During the sample period, the contribution of Theil index to carbon emission intensity decreased first and then increased. (4) From a geographical perspective, carbon emissions exhibit a pattern characterized by "high in the east, low in the west, dense in the north and sparse in the south". Therefore, establishing a sound regional carbon reduction cooperation mechanism and promoting green development tailored to local conditions have become the main direction for advancement.

Keywords: Carbon emission intensity; Extended Kaya model; Standard deviation ellipse model; Theil index model; Kernel density model

1. Introduction

China's rapid economic growth has been largely attributed to the development of traditional manufacturing industries. However, this growth model is characterized by high pollution and high resource input, representing an extensive approach to economic development, leading to ongoing issues including air pollution and environmental degradation. According to the IEA, China's carbon emissions in 2022 exceeded 11.14 million tons, indicating a slight 0.2% reduction from the previous year, yet the absolute amount still commands considerable attention. In order to avoid climate crisis, in 2022, the Chinese government formally proposed to the United Nations the "dual carbon" goal of "carbon peak by 2030 and carbon neutrality by 2060" (Yuan *et al.* 2023). In addition, the report of the 20th National Congress of the Communist Party of China repeatedly stressed that more measures should be taken to achieve the "dual carbon" goal (Chang 2022). Therefore, to facilitate the achievement of the "dual carbon" targets, it has become an urgent issue to conduct a comprehensive investigation on the spatial distribution pattern of carbon emissions across provinces in China and clarify the dynamic evolution of provincial carbon emissions.

Carbon emission has an important impact on economic development (Li *et al.* 2023; Zheng *et al*. 2023; Luo *et al.* 2023; Liu *et al.* 2024; Xu *et al.* 2023; Xu *et al.* 2024). Some scholars analyzed the carbon emission control mechanism from the perspectives of green building engineering, energy productivity, digitalization, waterway network, manufacturing transformation, technological innovation efficiency, sewage treatment, residential land transfer, etc. (Zhang *et al.* 2019; Zhang *et al.* 2023; Sun *et al.* 2024; Chen *et al.* 2024; Zhao *et al.* 2024; Qiu *et al.* 2024; Zhao *et al.* 2024; Liu, *et al.* 2024; Liu, *et al.* 2024). These studies provide significant references for the investigation of carbon emission issues.

Many scholars at home and abroad have paid attention to the efficiency of carbon emission intensity. Common methods involve parametric estimation or non-parametric estimation (Tao *et al.* 2022; Mohammad *et al.* 2021; Andrea *et al.* 2022; Blanchard 2021; Cai 2023; Liu 2024). Wu *et al*. (2022) calculated the carbon emission efficiency of crops in 30 provinces in China from 2001 to 2019 based on an extended relaxation-based measurement method. Zhang and Xi (2023) constructed a three-dimensional evaluation index system to evaluate the ecological environment and agricultural development in China's provinces based on the stage. The efficiency SBM model measures the efficiency of urban carbon emissions. Li *et al*. (2023) measured the carbon emission efficiency of the urban agglomerations in the Yangtze River Economic Belt, using the super-efficiency SBM model of undesirable output. Dussaux *et al*. (2023) analyzed the impact of third-country imports on France's domestic carbon intensity based on the shift-share instrumental variable method. Wei and Hengye (2022) utilized panel data to examine the impact of the first-order term of carbon emissions on carbon emission intensity. Zhang *et al*. (2022) used the super-efficiency three-stage data envelopment analysis model to measure the carbon emission intensity of Chinese agriculture from 2000 to 2019. Most of the aforementioned studies are based on the classic DEA model, proposing a multi-stage efficiency measurement method; however, these studies are primarily focused on the comparison of relative efficiency. Additionally, some scholars have used the stochastic frontier analysis models to measure carbon emission efficiency (Guo and Liang 2022; Xu 2022). Furthermore, there are scholars who have concentrated on the impact of environmental factors on carbon emission intensity, mainly employing econometric and statistical analysis models (Andrea *et al.* 2021; Li *et al.* 2023).

At present, the spatial analysis of carbon emissions has become a research frontier. Existing literature mainly focuses on issues such as carbon emission performance and characteristics, with primary research methods including trend analysis, Gini coefficient, and standard deviation ellipse. (Najul *et al.* 2022; Liu *et al.* 2022; Wang *et al.* 2023). On this basis, some scholars have used global spatial autocorrelation coefficients to reveal the spatial correlation of carbon emissions (Wei and Dong 2022; Zhou *et al.* 2023). In addition, some scholars have employed LISA time path, kernel density estimation, center-standard deviation ellipse, and other methods to analyze the spatiotemporal evolution characteristics of carbon emissions (Zhao *et al.* 2021; Liu and Wei 2022; Zhang 2023). Specifically, in terms of carbon emission performance, existing studies have indicated that China's carbon emissions have shown a fluctuating upward trend as a whole, with performance values changing from a low-value concentration and skewed distribution to a medium-value concentration and symmetric distribution (Cheng *et al.* 2023). Besides, China's carbon emissions demonstrate regional imbalances, with carbon emission performance presenting significant spatial disparities and pronounced spatial correlation characteristics, showing a distribution pattern of east > central > west (Hao *et al.* 2022). The polarization effect is significant in the Beijing-Tianjin-Hebei region and Yellow River basins. (Wang *et al.* 2023).

In summary, many scholars have conducted studies on the spatial distribution pattern and temporal evolution of carbon emissions at the regional, provincial (district and city), or county scale in China, yielding substantial results. However, the focus of these studies has been largely confined to specific regions, and the conclusions drawn from research data that is limited in scope and duration are inherently constrained, thereby precluding a holistic examination of the dynamic progression of China's carbon emission intensity. In view of this, the main objective of this paper is to analyze China's carbon emission intensity and its spatial characteristics. To clarify, this paper uses the standard deviation ellipse method to investigate the distribution characteristics of carbon emission spatial concentration in 30 provinces of China from 2005 to 2022. Subsequently, the Theil index is applied to characterize spatial differences, and ultimately, the kernel density model is employed to analyze the evolving trends.

The marginal contribution of this article lies in (1) Regarding the sample data, this study leverages carbon emission data from the CEADs database for China's 30 provincial regions to conduct a thorough examination of the distribution characteristics of China's carbon emission intensity. (2) In terms of research methods, this paper adopts the multi-method systematic analysis paradigm, using carbon emission intensity measurement, standard deviation ellipse, Theil index, kernel density and other models to systematically analyze the spatial effects of carbon emission intensity. (3) Concerning research value, the research conclusions of this article contribute to exploring carbon reduction pathways for Chinese provincial regions under diverse evolving trends, offering decision-making insights for the formulation of scientific inter-provincial carbon neutrality action plans that are adapted to China's new development pattern, thereby facilitating the achievement of China's dual carbon targets.

2. Materials and methods

2.1. Construction of Carbon Emission Intensity Measurement Model

Due to the lack of publicly disclosed carbon emission data from China’s official sources, most scholars index carbon emissions based on the Kaya model, with a principal focus on factors including economy, demography, and significant fuel consumption. The Kaya model was first proposed by Professor Yoichi Kaya, who has provided a specialized introduction to the method at a meeting of the United Nations Climate Change Conference. The model offers advantages including simple calculation, and elimination of the interference of residual and disturbance terms, effectively explaining the main factors affecting carbon emissions (Lv *et al.* 2016). The expression for calculating carbon emissions using the Kaya model is as follows (Du *et al.* 2022):

$$Q = p\times(\frac{Q_p}{E_p})\times(\frac{E_p}{P_{GD}})\times(\frac{P_{GD}}{P}) = p\times s\times i\times e \tag{2-1}$$

In the above equation, Q represents total carbon emissions, $E = E_p$ represents energy consumption, $G = P_{GD}$represents gross domestic product, P represents population size, $s=\frac{Q_p}{E_p}$ represents carbon dioxide emissions per unit of GDP, $i=\frac{E_p}{P_{GD}}$ represents energy input per unit of GDP, and $e=\frac{P_{GD}}{P}$ represents GDP per capita.

Further, according to the extended identity of the LMDIM obtained from the Kaya model, the residual value of the decomposition is obtained (Dai *et al.* 2015):

The residual value of the extended identity equation LMIDIM without decomposition

$$\Delta Q = Q_x - Q_y = \Delta Q_{pe} + \Delta Q_{ee} + \Delta Q_{ie} + \Delta Q_{se} \tag{2-2}$$

$$\Delta Q_{pe} = \frac{N_x - N_y}{InN_x - InN_y} In\frac{p_x}{p_y},$$

$$\Delta Q_{ee} = \frac{Q_x - Q_y}{InQ_x - InQ_y} In\frac{e_x}{e_y},$$

$$\Delta Q_{ie} = \frac{Q_x - Q_y}{InQ_x - InQ_y} In\frac{i_x}{i_y},$$

$$\Delta Q_{se} = \frac{Q_x - Q_y}{InQ_x - InQ_y} In\frac{s_x}{s_y},$$

Where ΔQ represents the difference in carbon emissions, and Q_x and $Q_y$represent the carbon emissions in year x and year y, respectively.ΔQ_{pe} represents population size, ΔQ_{ee} represents economic output effect, and ΔQ_{ie} and ΔQ_{se} represent energy substitution effect and energy structure effect respectively.

Carbon emission intensity usually refers to the amount of carbon emissions per unit of GDP. According to the Kaya model and its extended-expression, energy consumption and its effect function can be calculated. Therefore, the calculation formula for provincial carbon emission intensity is as follows (Zhao *et al.* 2017):

$$PCEI_{ij} = \frac{QprovEmission_{it}}{GDP_{it}} \tag{2-3}$$

Where, $PCEI_{ij}$ represents the carbon emission intensity of research object i, $QprovEmission_{it}$ represents the carbon emission of research object i in year t, and GDP_{it} represents the gross product of research object i in year t.

2.2. Construction of SDE model considering carbon emission differences

It is necessary to analyze the characteristics of carbon emission intensity from the perspective of space. In this paper, the standard deviation ellipse model (SDE) will be constructed. The strength of this model lies in its capacity to effectively distinguish the overall and discrete distributions of different factors in multiple directions (Xu *et al.* 2023).

According to relevant research, the standard deviation ellipse model can effectively calculate parameters including the distribution center, long-axis standard deviation, short-axis standard deviation, and azimuth angle of carbon emission intensity can be effectively calculated. The calculation formula is as follows (Liu *et al.* 2019):

(1) Spatial distribution center of gravity:

$$\overline{X}_c = \frac{\sum_{i=1}^{n}\omega_i x_i}{\sum_{i=1}^{n}\omega_i}, \overline{Y}_c = \frac{\sum_{i=1}^{n}\omega_i y_i}{\sum_{i=1}^{n}\omega_i} \tag{2-4}$$

(2) The standard deviations along the X-axis and Y-axis directions are, respectively:

$$\sigma_x = \sqrt{\frac{\sum_{i=1}^{n}(w_i\overline{x}_i\cos\theta - w_i\overline{y}_i\sin\theta)^2}{\sum_{i=1}^{n}w_i^2}} \tag{2-5}$$

$$\sigma_y = \sqrt{\frac{\sum_{i=1}^{n}(w_i\overline{x}_i\sin\theta - w_i\overline{y}_i\cos\theta)^2}{\sum_{i=1}^{n}w_i^2}}$$

(3) Azimuth angle:

$$\tan\theta = \frac{(\sum_{i=1}^{n}w_i^2\overline{x}_i^2 - \sum_{i=1}^{n}w_i^2\overline{y}_i^2) + \sqrt{(\sum_{i=1}^{n}w_i^2\overline{x}_i^2 - \sum_{i=1}^{n}w_i^2\overline{y}_i^2)^2 + 4\sum_{i=1}^{n}w_i^2\overline{x}_i^2\overline{y}_i^2}}{2\sum_{i=1}^{n}w_i^2\overline{x}_i\overline{y}_i} \tag{2-6}$$

In the above formula, $\overline{x}_I$, $\overline{y}_j$ represent the relative coordinates of the distance distribution center of gravity of the spatial location (x_i, y_j) respectively. w_i stands for weight. θ is the azimuth of the standard deviation ellipse

2.3. Construction of Theil index model of carbon emission intensity decomposition

This paper primarily investigates the spatial characteristics of carbon emission intensity at the provincial level. Since carbon emission intensity has eliminated the regional economic and demographic heterogeneities, the Theil index is commonly utilized to measure it. (Song and Lv 2017).

Theil index T is calculated using GDP proportion weighting. By conducting a first-order decomposition of the Theil index, the total national carbon emission difference can be decomposed into inter-regional and intra-regional differences across seven major regions: South China, Central China, Northeast China, Southwest China, North China, East China, and Northwest China. The formula for the total difference Theil index is as follows (Meng *et al.* 2018; Ren *et al.* 2022)

$$T_p = \sum_i\sum_j\left(\frac{Y_{ij}}{Y_i}\right)\log\left(\frac{Y_{ij}/Y}{p_{ij}/p}\right) \tag{2-7}$$

Where, Y_{ij} is the GDP of the j province in Region*i*. Y_i is the GDP of region i, P_{ij} is the carbon emission intensity of the j province in Region i. P_i is the total carbon emission intensity of region i. P is the total carbon emission intensity of the province. The inter-provincial differences that define region *i* are:

$$T_P = \sum_j (\frac{Y_{ij}}{Y_i}) \log\left(\frac{Y_{ij}/Y}{P_{ij}/P}\right) \tag{2-8}$$

Then the total difference can be decomposed by T_P into:

$$T_P = \sum_i \left(\frac{Yi}{Y}\right) T_P + \sum_j (\frac{Y_i}{Y}) \log\left(\frac{Y_i/Y}{P_i/P}\right) = T_{WR} + T_{BR} \tag{2-9}$$

Where T_{WR} is the difference within the region, T_{BR} is the difference among regions.

2.4. Construction of kernel density estimation model for analyzing spatio-temporal characteristics

To illustrate the continuous evolving trend of carbon emission structure in space, kernel density analysis is utilized to interpret the spatiotemporal evolution of carbon emission within Chinese provincial regions. Kernel density estimation method is a method of estimating unknown density function in probability theory (Wang and Wang 2015; Wang and Huang 2023).

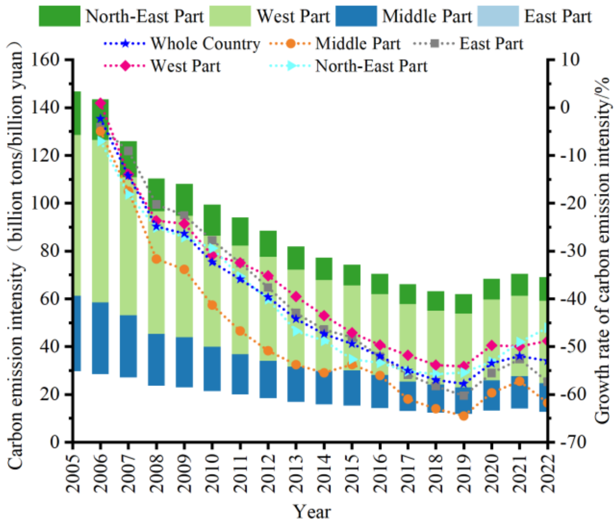

Figure 1. Growth rate of carbon emission intensity in different regions

The basic assumption of this method is that X_1, X_2, X_3, …, X_n follows n independent and equally distributed sample points, let the corresponding density function be $f(x)$; $f(x)$ is unknown and needs to be estimated by sample. The empirical distribution function of X_1, X_2, X_3, …, X_n is (Cui and Li, 2021; Lee *et al.* 2022; Luo *et al.* 2020):

$$f(x) = \frac{1}{n}\{X_1, X_2, \dots, X_n\} \tag{2-10}$$

The density estimation function can be obtained as follows:

$$f_h(x) = \frac{[F_n(x+h_n) - F_n(x-h_n)]}{2h} = \int_{x-h_n}^{x+h_n} \frac{1}{h} K\left(\frac{t-x}{h_n}\right) dF_n(t) = \frac{1}{nh}\sum_{i=1}^{n} K(\frac{X_i - x}{h_n}) \tag{2-11}$$

Where n is the total amount of carbon emission intensity data at provincial level; h is the bandwidth; k () is the kernel function; x_i is provincial carbon emission intensity, which belongs to independent and homogeneous distribution.

2.5. Sources of research data

The carbon emission data in this paper are mainly from CEAD s database (www.ceads.net), which primarily calculates carbon emissions based on the Kaya model and its improved methodologies. The study targets 30 provinces (municipalities and autonomous regions) in China. Tibet, Hong Kong, Macau and Taiwan are not considered due to lack of statistical data. Data for other variables are derived from authoritative publications such as China Statistical Yearbook and China Environmental Statistical Yearbook. Some missing data were completed by linear interpolation. In addition, due to the lag of the statistical yearbook, part of the 2022 data were supplemented by regression analysis.

3. Results

3.1. Carbon emission intensity measurement results

Based on the Kaya model and its improved model, statistical data were collected, and using MATLAB tools, the carbon emission intensity of 30 provincial regions in China from 2005 to 2022 can be calculated as shown in Table 1.

From the results, The intensity of carbon emissions shows a trend of first increasing and then decreasing. Although from 2005 to 2006, the intensity of carbon emissions remained relatively stable at 14.5 billion tons per billion tons, China's carbon emissions intensity has been steadily declining since a significant decrease in 2007, indicating that China's carbon emissions intensity indicator has been declining year by year due to technological progress and economic growth. 2020 and 2022 saw rebound in carbon emission intensity, which could be primarily attributed to two factors: the relaxation of environmental policies by the Chinese government in response to the COVID-19 from 2019, and the consequent surge in coal power generation due to electricity shortages.

As shown in Figure 1, from the regional perspective, since 2005, the carbon emission intensity in eastern region has decreased first, reaching a low point in 2019, with an emission volume of 1.18 billion tons/100 million yuan, accounting for about 19% of the country's total, but rebounding to 1.41 billion tons/100 million yuan in 2021. During the sample investigation period, the carbon intensity in the central and western regions both showed significant decreases, from 3.16 billion tons/100 million yuan to 1.12 billion tons/100 million yuan and from 6.72 billion tons/100 million yuan to 3.08 billion tons/100 million yuan accounting for 18% and 50% of the country's total emissions, respectively, rebounding to 1.35 billion tons/100 million yuan and 3.36 billion tons/100 million yuan in 2021. The change was most significant in Northeast China, where carbon emissions dropped from 1.82 billion tons per billion yuan in 2015 to 810 million tons per billion yuan in 2019, and finally rebounded to 990 million tons per billion yuan in 2022. Some regions experienced fluctuations in 2022, with the eastern and central regions dropping to 1.27 billion tons per billion yuan and 1.21 billion tons per billion yuan respectively.

3.2. Results of carbon emission intensity based on the standard deviation ellipse model

By ARCGIS calculation, typical time points are selected for analysis. According to Figure 2, the range of change in the distribution of the centroid of the ellipse is [110° 0′~110° 43′] E, [35° 52′~37°23′] N. Compared with the geometric center of China (103°E, 36°N), this time the centroid is shifting to the southeast. By examining the specific trajectory and direction of the change in the centroid of the standard deviation ellipse, within the scope of this investigation, the central point of China's carbon emission distribution moved from Xiangning County towards the northwest to Yonghe County, and then gradually shifted to the northeast. Consequently, the central point of carbon emissions is shifting to the northwest.

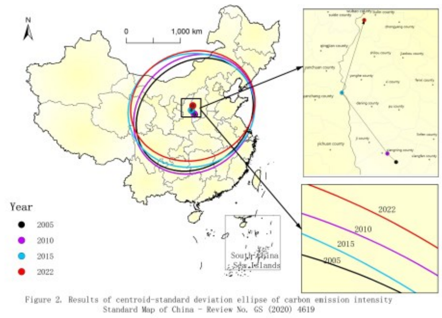

Figure 2. Results of centroid-standard deviation ellipse of carbon emission intensity

3.3. Decomposition results of carbon emission intensity based on Theil index

The previous analysis shows significant differences in carbon emissions among regions, with the distribution of carbon emission intensity demonstrating pronounced regional attributes. This warrants an in-depth examination of the factors contributing to the observed inter-regional emission differences. This article introduces the Theil index to measure the regional differences in carbon emission intensity. Compared to other methods, the Theil index makes it possible to observe the change between entities and their overall impact more clearly.

Through the first-order decomposition of Theil index, seven regional differences and inter-provincial differences in China's carbon emissions were analyzed. According to Table 2 and Figure 3, it can be seen that during the sample investigation period, China's carbon emission intensity differences showed an upward trend, from 0.1393 in 2010 to 0.2475 in 2019. The intra-provincial variation fluctuates around 0.15, which is the most important source of overall variation. The contribution rate of intra-group differences to the overall trend is increasing. According to the data from 2009 to 2022, the value of TBR is greater than that of TBP, and the value of TWP is negative. For example, the TBR value, TBP value and TWP value in 2022 are 0.2323, 0.1651 and -0.0553 respectively, and the Theil index value is 0.3421. Changes of Theil index in Figure 2 displays that the Theil index curve keeps increasing from 2009 to 2020, and slightly decreases from 2021 to 2022. This shows that the overall difference in carbon emission intensity has generally maintained an increasing trend.

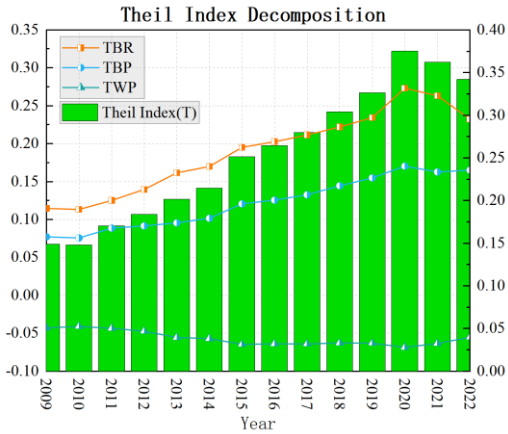

Figure 3. Decomposition value of the Theil index for carbon emissions across provincial regions in China – Line Chart

3.4. Spatial and temporal evolution results of carbon emission intensity based on kernel density estimation model

The evolution of carbon emission intensity is essentially a dynamic process of aggregation and diffusion among crucial regions. However, it is difficult for the above research to visually express the carbon emission change path in different provinces. Therefore, kernel density model is introduced for analysis.

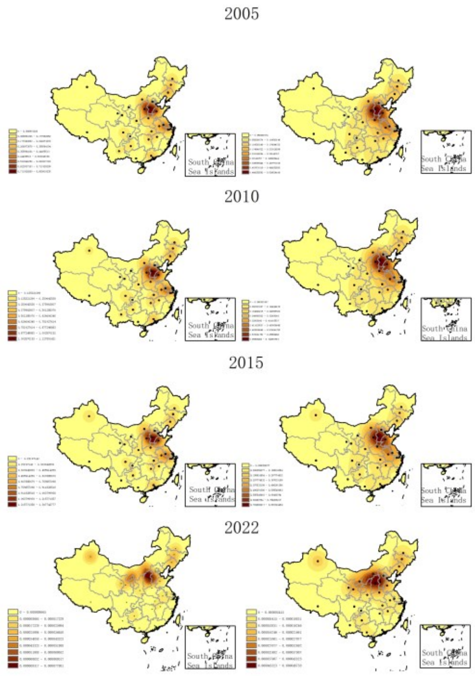

Figure 4. Spatial distribution pattern of carbon emission intensity across provincial regions in China in 2005, 2010, 2015, and 2022. Standard Map of China - Drawing Review No. GS (2020) 4619

As shown in Figure 4, according to the analysis of the evolution, the multi-scale bandwidth can reflect the spatiotemporal evolution of carbon emission intensity. On the whole, the Kernel density on the map is higher in the east than in the west, dense in the north and sparse in the south. In addition, there are also significant differences within the region, and the results are consistent with the previous findings.

Table 1. Carbon emission intensity of China's provinces (2005-2022)

Province	2005	2006	2007	2008	2009	2010	2011	2012	2013	2014	2015	2016	2017	2018	2019	2020	2021	2022
Beijing	1.68	1.47	1.26	1.13	1.06	0.93	0.75	0.69	0.57	0.54	0.49	0.42	0.38	0.35	0.32	0.32	0.33	0.35
Tianjin	3.93	3.74	3.39	2.71	2.64	2.70	2.49	2.25	2.12	1.92	1.85	1.66	1.52	1.47	1.41	2.10	2.26	1.51
Hebei	6.57	6.18	5.58	4.97	4.92	4.50	4.28	4.02	3.84	3.51	3.51	3.26	3.01	2.91	2.71	3.23	3.64	2.75
Shanxi Province	13.89	13.36	11.05	8.73	8.74	7.53	6.78	6.60	6.60	6.70	7.85	7.70	6.69	6.50	6.44	8.07	8.65	7.07
Inner Mongolia	8.85	12.11	8.20	8.07	7.72	7.38	7.98	7.49	6.73	6.46	6.01	5.71	5.56	5.89	6.13	8.43	7.52	7.62
Liaoning	6.73	6.29	5.52	4.89	4.79	4.84	4.40	4.17	3.74	3.59	3.44	3.45	3.34	3.28	3.38	3.82	4.42	4.65
Jilin	6.28	5.71	4.77	4.55	4.14	3.92	3.71	3.27	2.90	2.72	2.31	2.19	2.07	2.08	2.06	2.01	2.12	2.32
Heilongjiang	5.24	4.98	4.66	4.24	4.38	4.13	3.70	3.50	3.08	3.04	2.90	2.87	2.78	2.72	2.70	2.73	2.77	2.88
Shanghai	2.50	2.16	1.82	1.70	1.57	1.51	1.39	1.28	1.25	1.05	0.99	0.88	0.82	0.74	0.72	0.76	0.79	0.81
Jiangsu	2.65	2.47	2.18	1.86	1.75	1.62	1.59	1.47	1.37	1.25	1.17	1.12	1.00	0.92	0.88	0.89	0.91	0.93
Zhejiang	2.30	2.21	2.02	1.81	1.75	1.57	1.43	1.28	1.22	1.12	1.05	0.96	0.90	0.80	0.76	0.77	0.78	0.79
Anhui Province	3.46	3.24	2.96	2.83	2.73	2.37	2.07	1.92	1.86	1.75	1.66	1.50	1.38	1.25	1.16	1.18	1.20	1.22
Fujian	2.05	1.96	1.77	1.58	1.64	1.51	1.45	1.27	1.12	1.15	1.03	0.88	0.81	0.78	0.76	0.77	0.79	0.81
Jiangxi	2.97	2.72	2.42	2.05	1.95	1.84	1.65	1.50	1.45	1.34	1.31	1.21	1.12	1.04	0.98	0.99	1.01	1.03
Shandong Province	4.47	4.31	3.91	3.48	3.33	3.20	2.93	2.80	2.48	2.47	2.50	2.47	2.37	2.22	2.15	2.16	2.19	2.23
Henan Province	4.15	4.02	3.60	3.10	2.93	2.68	2.55	2.17	1.97	1.82	1.60	1.45	1.28	1.15	0.99	0.93	0.97	1.00
Hubei Province	3.74	3.60	3.18	2.57	2.41	2.24	2.07	1.83	1.41	1.28	1.13	1.03	0.94	0.87	0.85	0.83	0.87	0.91
Hunan Province	3.39	3.09	2.86	2.32	2.16	1.88	1.73	1.52	1.33	1.18	1.06	1.00	0.93	0.88	0.80	0.76	0.82	0.86
Guangdong Province	1.75	1.65	1.46	1.31	1.32	1.27	1.18	1.08	1.01	0.93	0.86	0.80	0.75	0.71	0.66	0.63	0.64	0.66
Guangxi	2.64	2.44	2.29	1.97	1.99	2.01	2.05	2.05	1.88	1.71	1.47	1.40	1.35	1.28	1.25	1.27	1.30	1.32
Hainan	1.84	2.38	3.64	3.16	3.06	2.68	2.59	2.39	1.98	1.98	2.01	1.78	1.57	1.52	1.44	1.59	1.75	1.86
Chongqing	3.10	2.98	2.65	2.25	2.14	1.95	1.76	1.53	1.18	1.12	0.90	0.82	0.76	0.71	0.66	0.65	0.68	0.71
Sichuan	3.19	2.98	2.69	2.34	2.36	2.01	1.66	1.52	1.41	1.34	1.09	0.98	0.84	0.73	0.72	0.75	0.79	0.85
Guizhou	8.53	8.39	7.21	6.00	5.97	5.14	4.57	4.17	3.66	3.07	2.67	2.50	2.18	1.78	1.67	1.76	1.87	1.96
Yunnan Province	5.05	4.75	4.00	3.47	3.45	3.10	2.60	2.31	1.98	1.63	1.38	1.25	1.18	1.16	1.09	1.04	1.09	1.13
Shaanxi	4.70	4.78	4.22	3.71	3.62	3.48	3.11	3.08	2.91	2.80	2.69	2.58	2.36	2.07	2.08	2.20	2.27	2.32
Gansu Province	6.94	6.27	5.75	5.10	4.73	4.36	4.13	3.80	3.52	3.27	3.15	2.87	2.73	2.59	2.43	2.43	2.47	2.51
Qinghai Province	5.39	5.40	5.16	4.53	4.40	3.61	3.56	3.81	3.74	3.24	2.74	2.85	2.50	2.19	2.02	2.05	2.13	2.21
Ningxia	12.71	11.81	10.21	8.78	8.68	8.28	8.97	8.73	8.51	8.15	8.11	7.49	8.00	8.13	8.28	8.45	8.58	8.70
Xinjiang	6.09	5.93	5.45	5.10	5.82	5.15	5.00	5.09	5.15	5.19	5.33	5.38	4.94	4.48	4.49	4.76	4.96	5.08

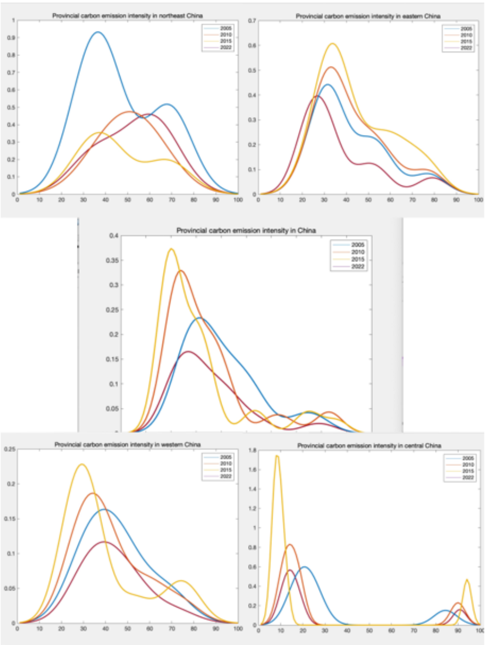

Figure 5. Distribution of carbon emission intensity across provincial regions in China

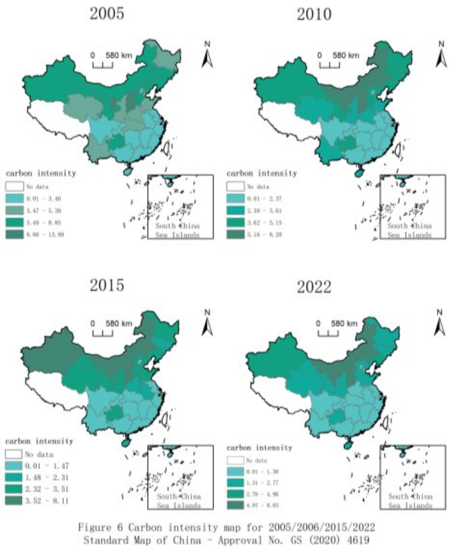

Figure 6. Spatial distribution of carbon emission intensity across different provinces

Further, the variations of regional Kernel density curves in 2005, 2010, 2015 and 2022 were plotted respectively, as shown in Figure 5. Taking the central region as an example, the Kernel density curve in 2022 first increased and then decreased, and subsequently increased again before decreasing, showing the characteristics of "U-shaped" and "inverted U-shaped" changes, with consistent patterns observed in the year 2005, 2010, and 2015. The national trend, along with those of the eastern, western, and northeastern regions, has exhibited similar patterns of change. Consequently, an examination of evolution trend of carbon emission intensity across China and its four regions, with focus on the curve's positioning, span, and peak value, indicates pronounced spatial and temporal heterogeneity in carbon emission intensity.

4. Discussion

4.1. Further discussion on changes in carbon emission intensity

The results of carbon emission intensity were calculated based on the Kaya model and its improved model. To compare the trends in different time series from 2005 to 2022 in China, the map in Figure 6 was drawn using ArcGIS software.

Referring to relevant studies (Kamani *et al.* 2023), as shown in Figure 6, in terms of the growth rate of carbon intensity, the trend in the growth rate of carbon emissions across China's provincial regions has been on a downward trajectory from 2006 to 2019. Furthermore, aside from the western region experiencing a positive growth rate in 2006, all other regions have shown a negative growth in carbon intensity in all subsequent years. From 2020 to 2022, the growth rate of carbon emissions saw a resurgence. Regarding the growth rate of carbon intensity, except for a fluctuating rebound in the central region in 2015, all other areas showed a downward trend. Based on the results, it can be seen that the intensity of carbon emissions is significantly affected by economic growth and policy measures. In 2020, when the Chinese government proposed the strategic goal of "carbon peak by 2030", the intensity of carbon emissions rebounded, illustrating that 2020 was a significant turning point.

Table 2. Decomposition value of the Theil index for carbon emissions across provincial regions in China

Years	TBR	TBP	TWP	Theil index
2009	0.1147	0.0772	-0.0428	0.1490
2010	0.1133	0.0757	-0.0411	0.1479
2011	0.1251	0.0886	-0.0435	0.1702
2012	0.1396	0.0916	-0.0473	0.1839
2013	0.1615	0.0956	-0.0555	0.2015
2014	0.1700	0.1017	-0.0570	0.2147
2015	0.1952	0.1207	-0.0646	0.2513
2016	0.2025	0.1257	-0.0638	0.2644
2017	0.2114	0.1326	-0.0641	0.2798
2018	0.2220	0.1445	-0.0627	0.3038
2019	0.2344	0.1549	-0.0631	0.3262
2020	0.2732	0.1705	-0.0685	0.3751
2021	0.2631	0.1627	-0.0634	0.3624
2022	0.2323	0.1651	-0.0553	0.3421

Table 3. Theil contribution values of carbon emissions by region from 2009 to 2022

Year	Northeast	East China	Central China	North China	South China	Northwest	Southwest
2009	0.0018	0.0398	0.0081	0.1892	0.0571	0.0488	0.0887
2010	0.0042	0.0410	0.0104	0.1799	0.0433	0.0568	0.0839
2011	0.0034	0.0373	0.0125	0.2035	0.0469	0.0805	0.0903
2012	0.0055	0.0439	0.0103	0.2109	0.0486	0.0766	0.0948
2013	0.0061	0.0384	0.0157	0.2179	0.0395	0.0808	0.1029
2014	0.0066	0.0476	0.0189	0.2323	0.0452	0.0881	0.0826
2015	0.0128	0.0583	0.0170	0.2597	0.0550	0.1039	0.0960
2016	0.0167	0.0721	0.0154	0.2778	0.0480	0.0964	0.1025
2017	0.0183	0.0778	0.0117	0.2736	0.0423	0.1263	0.0951
2018	0.0167	0.0810	0.0091	0.2837	0.0445	0.1542	0.0753
2019	0.0199	0.0819	0.0042	0.2996	0.0484	0.1693	0.0722
2020	0.0340	0.0789	0.0036	0.3090	0.0634	0.1688	0.0799
2021	0.0474	0.0778	0.0024	0.2864	0.0730	0.1659	0.0824
2022	0.0443	0.0767	0.0018	0.3256	0.0776	0.1633	0.0815

4.2. Discussion on the decomposition of carbon emission intensity based on Theil index

Theil index is instrumental in assessing assess regional differences in carbon emissions. Beyond analyzing the differences in carbon emission intensity at the provincial level, it is also necessary to adopt a regional clustering method to compare the spatial differences in China's carbon emissions (Kamani 2023). According to the clustering results, the sample data is reclassified to obtain the carbon emission intensity of different regions.

As shown in Table 3, during the study period, the overall difference in carbon emission intensity among the seven regions has increased, while the contribution rate of the Theil index from 2010 to 2017 to the overall Theil index has been decreasing year by year. Between 2018 and 2019, the contribution rate of inter-regional carbon emissions has surpassed that within regions. According to the actual mean value of the Theil index contribution regarding the inter-provincial carbon emission differences from 2010 to 2022, it can be deduced that: North China>Northwest>Southwest>EastChina>SouthChina>Northeast>Central China.

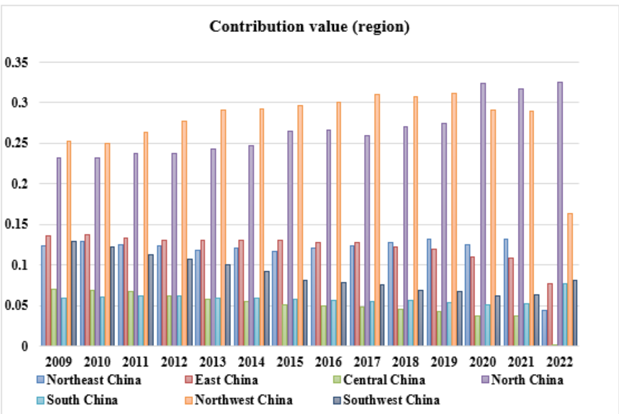

Figure 7. Theil contribution values for carbon emissions across regions in China–Bar Chart

As shown in Figure 7, the mean value of Thiel contribution is 0.170 in Northeast China, 0.609 in East China, 0.1011 in Central China, 0.2535 in North China, 0.0523 in South China, 0.1128 in Northwest China, and 0.0877 in Southwest China. North China tops the values, with Central China at the bottom. This indicates significant disparities in carbon emissions among regions, with pronounced differences within provinces. In addition, according to the contribution rate index, East China is the highest, all above 70%; South China is the lowest, less than 10%.

Figure 8 further demonstrates the distribution of Theil contribution values of different provinces, plotting the distributions in 2012, 2014, 2016, 2018, 2020 and 2022. From the results, the Thiel index shows certain changes in different years, especially the farther away from the year, the more significant the change. This test further verifies the typical characteristics of spatial heterogeneity of China's carbon emissions.

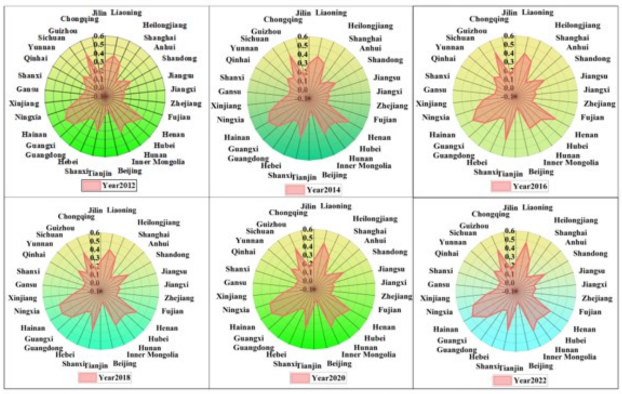

Figure 8. Map of Theil contribution value of carbon emissions in different provinces (2012-2022)

4.3. Discussion of carbon emission intensity results based on kernel density estimation model

The distribution curve of kernel density estimation is plotted as shown in Figure 8 to further compare the carbon emission characteristics of different regions.

As shown in Figure 8, considering the position of the curves, the centers of the kernel density functions for the three regions excluding the Northeast, as well as the national trend, have shown a tendency to move to the left and then to the right between 2005 and 2021. In the Northeast region, the peak shifted from a bimodal to a unimodal pattern between 2005 and 2010, indicating a reduction in polarization. Among them, the changes in the western region were more pronounced. In contrast, the changes in the whole country and the eastern region were relatively small, indicating that the magnitude of changes in carbon emission intensity across various regions was inconsistent. Furthermore, the kernel density tends to move towards lower values.

From the peak change of the curve, the peak density of all regions showed a decline from 2005 to 2015. The shape of the density function curve in the eastern, western and central regions and the whole country shifted from a sharp peak to a broader peak, while the Northeast region exhibited a trend of narrowing from a broad to a sharp peak. This indicates that the carbon emission intensity in different regions presents U-shaped and inverted U-shaped changes. Finally, upon examining the results from 2016 to 2022, the variations in the curves across different regions have narrowed, showing dynamic convergence. Possible reasons: With the concept of green development, the Chinese government has introduced a series of policies to reduce carbon emissions, effectively suppressing the growth of carbon emission intensity.

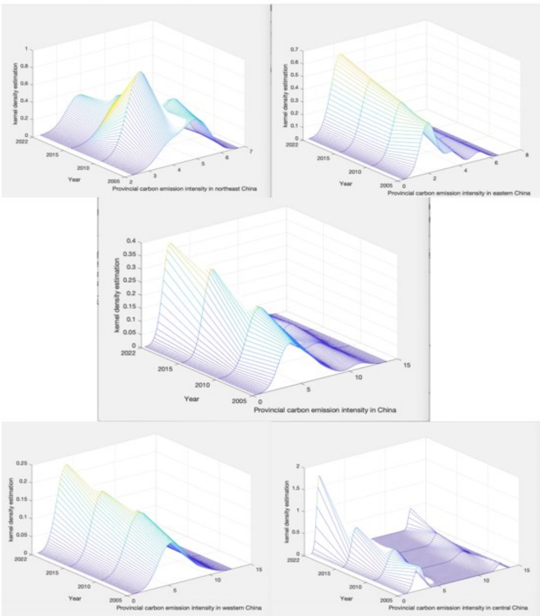

Figure 8. Distribution Curves of Carbon Emission Kernel Density Estimation in Different Regions

5. Conclusion

Based on the typical fact that "reducing carbon emissions" can promote the low-carbon circular development of the economy and society, this article uses panel data from 2005 to 2022 to analyze the impact of carbon emission reduction on China's economic growth, industrial structure, and energy consumption. This article systematically analyzes the carbon emission intensity of provinces in China, thoroughly examining the intensity characteristics, regional spatial disparities, and the trends of spatiotemporal evolution. The principal research findings are as follows:

First, from a holistic perspective, the distribution of carbon emission intensity in China is characterized by significant regional heterogeneity, with significant differences in emissions among regions. The distribution of the centroid of the geometric ellipse of China varies from [110°0′～110°43′] E, [35°52′～37°23′] N, indicating that the carbon emission intensity in eastern and southern China is higher than that in western and northern China.

Secondly, resulting from technological progress and economic growth during the sample period, the overall difference in China's carbon emission intensity decreased yearly but showed a "U" shaped fluctuation trend. In terms of carbon emission intensity, the carbon intensity of the eastern region rebounded to 1.41 billion tons per billion yuan in 2021 and dropped back to 1.27 billion tons per billion yuan in 2022. In 2019, the figure for central region dropped to 1.12 billion tons/billion yuan, rebounded to 1.35 billion tons/billion yuan in 2021, and dropped back to 1.21 billion yuan in 2022. In 2019, the carbon intensity of the western region fell to 3.08 billion tons/billion yuan, and rebounded to 3.36 billion tons/billion yuan in 2021. The carbon intensity of the Northeast region in 2019 was 810 million tons/billion yuan, and it rebounded to 990 million tons/billion yuan in 2022, making the Northeast region the area with the lowest carbon intensity.

Thirdly, according to the test results, regional differences have a significant impact on carbon emissions. The Theil index decomposition results reveal that inter-regional carbon emission disparities were less pronounced than intra-regional differences from 2010 to 2017, yet exceeded them from 2018 to 2022. This trend highlights the necessity for provinces to harness the carbon trading market's potential in reducing carbon emissions.

Fourthly, from the perspective of the national spatial pattern of provincial carbon emissions, the spatial distribution of provincial carbon emissions in China shows a trend of "high in the east and low in the west, dense in the north and sparse in the south". From 2005 to 2015, the kernel density curve showed a downward trend in general, with the centers of carbon emission kernel density functions in various regions showing distinct patterns of convergence. The spatial evolution of carbon emission intensity in different regions during 2016-2022 showed a decreasing trend, indicative of dynamic convergence. At the same time, according to the two-dimensional and three-dimensional curves of the kernel function, it is found that the carbon emission distribution in different regions generally presents a trend from agglomeration to dispersion. However, in 2022, the national and western regions experienced a weakening in their concentration trends; the spatial disparity in carbon intensity within the central region gradually diminished; and the Northeast region saw a transition from a bimodal to a unimodal peak in its curve, indicating a decline in polarization.

The above conclusions hold important theoretical and practical value. At the existing policy level, it is necessary to combine the carbon emission differences and economic development status of different regions, give priority to the implementation of carbon trading system for eastern provinces and cities with large carbon emissions and economically developed enterprises, and promote the green economic transformation. Moreover, it is crucial for the national government to set reasonable emission reduction targets for all provinces and cities, and allocate carbon emission quotas for different regions according to the development status of different provinces and cities. To establish a complete unified carbon trading market, it is also necessary to consider the carbon intensity of neighboring provinces, establish a sound regional carbon emission reduction cooperation mechanism, and advance the green development of provinces in accordance with local conditions.

Ethics approval and consent to participate

Not applicable.

Consent for publication

Not applicable.

Availability of data and materials

Not applicable.

Competing interests

The authors have no conflicts of interest to declare.

Funding

This research was funded by 2023 National Foreign Experts Project of the Ministry of Science and Technology of China (No. DL2023202002L), by Tianjin art science planning general project（No. B24017), by China Civil Aviation High-quality Development Research Center 2023 open fund key project (No. ADI2023-1-02).

Authors' contributions

Gang Zeng, Yi Guo, Song Nie: Conceptualization, Investigation, Resources, Writing –original draft, review & editing. Keyan Liu, Yue Cao, Ling Chen, Dezhe Ren: Writing – original draft, Writing – review & editing. Jiaqi Zhang, Bowen Yan: Writing – review & editing.

Authors' information (optional)

Not applicable.

Acknowledgements

Not applicable.

References

Andrea F., Nastia D., Ivana M., *et al*. (2021). Greenhouse gas emissions reduction potential by using antifouling coatings in a maritime transport industry. *Journal of Cleaner Production*, **295**.

Andrea F., Nastia D., Ivana M., *et al*. (2022). Energy savings potential of hull cleaning in a shipping industry. *Journal of Cleaner Production*, 2022: 374.

Chang Y.M. (2022). The logical approach, connotation, and practical application of promoting the "dual carbon" work in the report of the 20th CPC National Congress. *Environment and Development*, 1–6+21.

Chen J., Wang H., Yin W. *et al*. (2024). Deciphering carbon emissions in urban sewer networks: Bridging urban sewer networks with city-wide environmental dynamics. *Water Research*, 121576.

Cheng Y., Zhang Y. and Wang J.J. (2023). China Provincial Carbon Emissions Research on the Spatiotemporal Evolution of Performance and Technology Innovation Driving. *Geographical Science*, 313–323.

Cui R. and Li G.F. (2021). Regional disparities and dynamic evolution of China's Internet development level: 2006–2018. *Journal of Quantitative Economics and Technology Economics*, 3–20.

Cui Y., Su W., Xing Y., Hao L., Sun Y. and Cai Y. (2023). Experimental and simulation evaluation of CO_2/CO separation under different component ratios in blast furnace gas on zeolites. *Chemical Engineering Journal*, 144579.

Dai X.W., He Y.Q. and Zhong Q.B. (2015). Analysis of driving factors of China's agricultural carbon emissions based on the extended Kaya identity. *Journal of University of Chinese Academy of Sciences*, 751–759.

Du H.B., Zhao L.J., Liu C.W. *et al*. (2022). Urban Areas Based on LEAP Model and KAYA Model Carbon peak prediction and uncertainty analysis. *Journal of Ecology and Rural Environment*, 983–991.

Dussaux D., Vona F., Antoine D. (2023). Imported carbon emissions: Evidence from French manufacturing companies. *Canadian Journal of Economics/Revue canadienne d'économique*, 593–621.

Guo P. and Liang D. (2022). Does the low-carbon pilot policy improve the efficiency of urban carbon emissions: Quasi-natural experimental research based on low-carbon pilot cities. *Journal of Natural Resources*, 1876–1892.

Hai C.X., Yan L.L., Ying J.Z. *et al*. (2022). Analysis of spatial associations in the energy–carbon emission efficiency of the transportation industry and its influencing factors: Evidence from China. *Environmental Impact Assessment Review*, **97**.

Hao Y.W., Han J.H., Wen K.C. *et al*. (2022). Estimation and spatiotemporal analysis of the carbon-emission efficiency of crop production in China. *Journal of Cleaner Production*, **371**.

Jian H., Lin C. and Na Z. (2022). A Statistical Review of Considerations on the Implementation Path of China's Double Carbon Goal. *Sustainability*, 11274–11274.

Jin P.L. and De L.W. (2022). Analysis on the dynamic evolution of the equilibrium point of carbon emission penetration for energy-intensive industries in China: based on a factor-driven perspective. *Environmental science and pollution research international*, 5178–5196.

Kamani H., Baniasadi M., Abdipour H., Mohammadi L., Rayegannakhost S., Moein H. and Azari A. (2023). Health risk assessment of BTEX compounds (benzene, toluene, ethylbenzene and xylene) in different indoor air using Monte Carlo simulation in zahedan city, Iran. *Heliyon*

L C.B., L S.S., S E.E. *et al*. (2021). Ambient PMsub2.5/sub Organic and Elemental Carbon in New York City: Changing Source Contributions During a Decade of Large Emission Reductions. *Journal of the Air Waste Management Association*, 995–1012.

Lee J., Lumley D. and Lim U.Y. (2022). Improving total organic carbon estimation for unconventional shale reservoirs using Shapley value regression and deep machine learning methods. AAPG Bulletin.

Li B., Wang J., Nassani A. A. *et al*. (2023). The future of Green energy: A panel study on the role of renewable resources in the transition to a Green economy. *Energy Economics*, 107026.

Li L., Zhang B., Xia Q.Y. *et al*. (2023). The spatial effect of mismatched carbon emission efficiency of land resources and its impact path: empirical evidence from 108 cities in the Yangtze River Economic Belt. *Resources Science*, 1059–1073.

Li Z., Yang Y., So N. *et al*. (2023). Carbon footprint of maize planting under intensive subsistence cultivation in South Korea. *International Journal of Climate Change Strategies and Management*, 301–321.

Liu H.J., Wang Y.H. and Lei M.Y. (2019). Spatial Agglomeration and Evolution of China's Strategic Emerging Industries. *Journal of Quantitative Economics and Technology Economics*, 99–116.

Liu X., Zhu C., Kong M. *et al*. (2024). The Value of Political Connections of Developers in Residential Land Leasing: Case of Chengdu, China. *Sage Open*.

Liu X., Zhu C., Kong M., Yin L. and Zheng W. (2024). The Value of Political Connections of Developers in Residential Land Leasing: Case of Chengdu, China. *Sage Open*.

Liu Z., Xu Z., Zhu X. *et al*. (2024). Calculation of carbon emissions in wastewater treatment and its neutralization measures: A review. *Science of The Total Environment*, 169356.

Liu Z., Zhao Y., Wang Q. *et al*. (2024). Modeling and Assessment of Carbon Emissions in Additive-Subtractive Integrated Hybrid Manufacturing Based on Energy and Material Analysis. *International Journal of Precision Engineering and Manufacturing-Green Technology*.

Luo J., Zhuo W., Liu S. *et al*. (2024). The Optimization of Carbon Emission Prediction in Low Carbon Energy Economy Under Big Data. IEEE Access, 14690–14702.

Luo X., Ao X., Zhang Z. *et al*. (2020). Spatiotemporal variations of cultivated land use efficiency in the Yangtze River Economic Belt based on carbon emission constraints. Journal of Geographical Sciences, 535–552.

Lv Y. and Chen Z.Q. (2016). Research on Energy Consumption, Nitrogen Emissions and Their Influencing Factors in Zhejiang Province Based on Kaya Expansion. *Journal of Zhejiang University: Science Edition*, 610–615+624.

Meng L.X., Yang C.H., Li H.B. *et al*. (2018). Analysis of regional differences in water pollutant emission intensity in China based on Theil index. *Environmental Pollution and Control*, 241–246.

Mohammad Z., Mehdi P., Ali M.F. *et al*. (2021). A highly carbon‐efficient and techno‐economically optimized process for the renewable‐assisted synthesis of gas to liquid fuels, ammonia, and urea products. *International Journal of Energy Research*, 16362‐16382.

Najul L., Nikhil K., Chandra P.B. *et al*. (2022). Carbon emission intensity and firm performance: An empirical investigation in Indian context. *Journal of Statistics and Management Systems*, 1073–1081.

Qiu L., Yu R., Hu F. *et al*. (2023). How can China's medical manufacturing listed firms improve their technological innovation efficiency? An analysis based on a three-stage DEA model and corporate governance configurations. *Technological Forecasting and Social Change*, 122684.

Song L. and Lv J. (2017). Measuring the Regional Differences in Environmental Regulation Intensity in China Based on Theil Index. *Shandong Social Sciences*, 140–144.

Sun C., Chen J., He B. *et al*. (2024). Digitalization and carbon emission reduction technology R D in a Stackelberg model. *Applied Economics Letters*, 1–6.

Tao F., Debin F. and Bolin Y. (2022). Carbon emission efficiency of thermal power generation in China: Empirical evidence from the micro-perspective of power plants. *Energy Policy*, **165**

Wang H. and Wang S.Q. (2015). Dynamic evolution and spatial spillover effect of China's industrial CO_2 emission performance. China Population, Resources and Environment, 2015: 29–36.

Wang S.B., Zhuang G.Y. and Dou X.M. (2023). Province of China Domain carbon Peak-echelon division and differentiated emission path: an investigation based on the dual perspectives of carbon emissions and economic development. *Wuhan University* (Philosophy and Social Sciences Edition), 2023: 136–150.

Wang Z.F. and Huang D.C. (2023). Comparison of Carbon Emission Efficiency of Transportation in the Yangtze River Economic Belt and the Yellow River Basin and Its Influencing Factors. China Population, *Resources and Environment*, 2023: 1–15.

Wei S. and Hengye D. (2022). Measurement of provincial carbon emission efficiency and analysis of influencing factors in China. *Environmental science and pollution research international*, 38292–38305.

Wei S. and Hengye D. (2022). Measurement of provincial carbon emission efficiency and analysis of influencing factors in China. *Environmental science and pollution research international*, 38292–38305.

X Z., X Z. and K L. (2022). Regional differences and dynamic evolution of China’s agricultural carbon emission efficiency. *International Journal of Environmental Science and Technology*, 4307–4324.

Xiao H.L., Xiang Y.T., Yao W. *et al*. (2022). Improving carbon emission performance of thermal power plants in China: An environmental benchmark selection approach. *Computers Industrial Engineering*, **169**.

Xu A., Song M., Wu Y. *et al*. (2024). Effects of new urbanization on China's carbon emissions: A quasi-natural experiment based on the improved PSM-DID model. *Technological Forecasting and Social Change*, 123164.

Xu H., Yang C., Li X. *et al*. (2024). How do fintech, digitalization, green technologies influence sustainable environment in CIVETS nations? An evidence from CUP FM and CUP BC approaches. *Resources Policy*, 104994.

Xu L.L., Shu L.C., Li W. *et al*. (2023). Spatial and temporal evolution characteristics of groundwater extraction in China from 2000 to 2020.*Water Resources Protection*, 2023: 79–85+93.

Ya Y.Z., Rui Y.C., Peng Z. *et al*. (2021). Spatiotemporal patterns of global carbon intensities and their driving forces. *The Science of the total environment*, 2021: 818151690–151690.

Yu F.R., Wan R.Y., Bi T.Z. *et al*. (2022). Does improvement of environmental efficiency matter in reducing carbon emission intensity? Fresh evidence from 283 prefecture-level cities in China. *Journal of Cleaner Production*, **373**

Yuan X.l., Yang Y., Sheng X.R. *et al*. (2023). Carbon peak Analysis of the Neutralization Policy and countermeasures. Journal of Shandong University (Engineering Edition), 2023: 132–141.

Zhang M.d. and Xi S.J. (2023). Evaluation of carbon emission efficiency of resource-based cities and its policy enlightenment. *Journal of Natural Resources*, 220–237.

Zhang R., Yin L., Jia J., *et al*. (2019). Application of ATS-GWIFBM Operator Based on Improved Time Entropy in Green Building Projects. *Advances in Civil Engineering*, 3519195.

Zhang Y.Y., Chen F.Y., Xu X. *et al*. (2023). Analysis of carbon emission effects of land use in Fujian Province based on county scale. *Environmental Science Research*, **36**, 1446–1456.

Zhao F.W. and Hai Q.S. (2023). Spatiotemporal differences in and influencing factors of urban carbon emission efficiency in China's Yangtze River Economic Belt. *Environmental science and pollution research international.*

Zhao G.M., Zhao G.Q., Chen L.Z. *et al*. (2017). Spatial and temporal evolution and transition mechanism of China's carbon emission intensity. C*hina Population, Resources and Environment*, 2023: **27**, 84–93.

Zhao S., Zhang L., An H. *et al*. (2023). Has China's low-carbon strategy pushed forward the digital transformation of manufacturing enterprises? Evidence from the low-carbon city pilot policy. *Environmental Impact Assessment Review*, 107184.

Zhao S., Zhang L., Peng L. *et al*. (2024). Enterprise pollution reduction through digital transformation? Evidence from Chinese manufacturing enterprises. *Technology in Society*, 2024: 102520.

Zheng C. and Chen H. (2023). Revisiting the linkage between financial inclusion and energy productivity: Technology implications for climate change. *Sustainable Energy Technologies and Assessments*, 103275.

Zheng S., Hai Q., Zhou X., *et al*. (2024). A novel multi-generation system for sustainable power, heating, cooling, freshwater, and methane production: Thermodynamic, economic, and environmental analysis. *Energy*, 2023:130084.

Zhou C.Y., Wang Z., Zheng Y., *et al*. (2023). A study on the spatial differentiation of carbon amounts in the county’s Collaborative Carbon Control Alliance from the perspective of scaling reorganization—an analysis based on the carbon reduction potential of Zhejiang Province. *Geographic Research*, 2023: 1545–1559.